An isotopic study on oxygen uptake/exchange over ceria-praseodymia mixed oxides with pulse experiments using $^{18}O_2$: Implications on soot combustion activities in the GDI (Gasoline Direct Injection) context

Juan Carlos Martínez-Munuera [a], Marina Cortés-Reyes [b], Avelina García-García [a,*]

[a] MCMA Group, Department of Inorganic Chemistry and Institute of Materials, University of Alicante, San Vicente del Raspeig E-03690, Spain
[b] Departamento de Ingeniería Química, Facultad de Ciencias, Campus de Teatinos, Universidad de Málaga, Málaga E-29071, Spain

A B S T R A C T

This research work focuses on a preliminary study of the behaviour of several ceria-praseodymia mixed oxides along with three model catalysts under isotopic oxygen pulses at different temperatures in an attempt to investigate their ability to interact with $^{18}O_2$ (uptaking/releasing/exchanging) with their own lattice oxygen, under conditions which could simulate those existing in GDI exhaust gases. Furthermore, these ceria-praseodymia mixed oxides were studied to explore their responses towards soot combustion under two consecutive $^{18}O_2$ pulses at 500 °C. It was observed that the capacity of oxygen activation and uptake is very dependent on the nature of the catalyst. $Ce_{1-x}Pr_xO_{2-\delta}$ catalysts present different responses in the O_2 activation and uptake processes, as a function of temperature, praseodymium content and method of preparation. Moreover, some of these ceria-praseodymia formulations exhibited high soot combustion activity with a marked intervention of unlabelled active oxygen species during the inert period after the $^{18}O_2$ pulse.

1. Introduction

Due to their improved fuel efficiency, an increase in European and US market penetration for Gasoline Direct Injection (GDI) vehicles, is expected in a near future [1]. However, the use of GDI engines also carries unintended consequences, including significantly higher particulate emissions when compared to port-fuel injection (PFI) engines. These consist, mainly, in fine particles (broadly in the 10–100 nm size range). While the emissions may be low on a mass basis, these can be very high (10^{11}-10^{13} particles/km) on a number basis. These numbers of particles emitted per kilometre are more than an order of magnitude higher than for PFI engines, exceeding the tailpipe limit of $6 \cdot 10^{11}$ particles/km in Europe and China [2,3]. The ambient ultrafine particulate matter concentrations have a major impact on human health [4] with an increase in all-cause cardiovascular and respiratory mortality (along several ranges) [5].

A first approach to tackle these soot emissions is to incorporate a Gasoline Particulate Filter (GPF) downstream the Three-Way Catalyst (TWC) in the exhaust [2,6]. However, to avoid severe problems such as growing back pressure due to soot deposition onto the filter, this device should be regularly regenerated. One practical method would be periodically raising the temperature of the GPF to above 600 °C. However, uncontrolled soot combustion can lead to uncontrollable exothermic and filter damage [3,6]. A catalysed gasoline particulate filter (cGPF) could decrease the soot ignition temperature in a controlled fashion and thereby increase the service life of this device. For this reason, it is necessary to design efficient catalysts for the application of cGPF [7,8].

Unfortunately, the typical conditions of the exhaust are very unfavourable for soot combustion: essentially, there is no NO_2 due to the expected high efficiency of TWC and O_2 is only available during short pulses (due to fuel cuts, such as decelerations), independently on the modes of vehicle operations. In other words, more or less frequent short fuel cuts motivated by different modes of operation (city or highway driving) lead to transient oxygen concentration which means the occurrence of very short O_2 pulses separated by (free-oxygen) atmosphere periods [9]. These particular conditions (very far from those found in traditional and modern diesel exhausts) can become conventional diesel oxidation catalysts (e.g. based on platinum) quite ineffective [7,10].

In this demanding context, catalysts that exhibit high Oxygen Storage Capacity (OSC) should be very interesting for regeneration purposes.

---

* Corresponding author.
  E-mail address: a.garcia@ua.es (A. García-García).

They should present high capacity for incorporating oxygen during the short pulses under low/medium concentration of oxygen, and an accentuated ability to a complete release of O_2 during the long periods under non-oxidant atmosphere. The ability of ceria-based materials to promote oxygen storage/redox behaviour is behind their application as practical soot oxidation catalysts under O_2 [11–13]. Therefore, catalysts which could assist soot oxidation under highly transient conditions (long periods with no O_2 supply if the upstream TWC works under stoichiometric conditions) will be demanded [14]. This means that catalysts that lose their surface/subsurface and bulk oxygen very easily, creating a sufficient "active oxygen" supply (generating a large population of oxygen vacancies) and, concurrently, with fast kinetics of vacancies reoxidation during the very short oxygen pulses, will be the materials potentially suitable for these special and hard-working conditions of cGPF operation.

In the very recent years, some papers focused on catalytic materials for GPF have been published in the literature [7,8,14–24]. Specifically, two sets of catalysts' families have been investigated. On one hand, doped-perovskites [15,16] are claimed to be suitable to oxidise soot at low oxygen pressures, due to their redox properties and oxygen surface vacancies, by transporting bulk oxygen to the catalyst-soot contact points. On the other hand, ceria-based catalysts [7,8,14,18–22] could also be very interesting for this application due to their OSC and unique redox properties, thus showing abilities to rapidly modifying their oxidation state from Ce^{4+} to Ce^{3+} and contributing to the mechanism of soot oxidation by promoting the formation of oxygen vacancies at the interface between ceria and carbon, which is the key point to obtain active surface oxygen species [8]. In this context, special attention deserves the smart works reported by Liu, Wu and co-workers [18–20], who found that a large variety of $Ag/M_xO_y/Ce$ materials can be considered promising catalysts under typical conditions of gasoline engines due to bulk-to-surface oxygen migration processes, with tandem oxygen delivery routes, resulting in highly efficient transfer of bulk oxygen to soot.

In a previous work of some of the authors [14], it was reported that the praseodymium incorporation onto the ceria enhanced the oxygen mobility in the surface/bulk of the sample favouring higher O_2 released amounts under inert atmosphere with regard to ceria. The efficiency of the own active oxygen species released from the catalyst to oxidise soot under inert atmosphere, even under loose contact mode, was well demonstrated. In a singular way, at high temperatures under loose contact mode, soot could act as a "driving force" and the "own lattice oxygen" could be transferred directly towards soot surface efficiently [14,25].

Based on these initial premises, Pr-doped cerias can constitute interesting materials to be tested as catalysts in the special conditions demanded by cGPF applications. In this sense, together with Ag-perovskites [16], Ag promoted Fe_2O_3 @CeO_2 [20] and Co_3O_4-CeO_2 [22] can constitute other competitive formulations in the new generation of oxygen deliverers catalysts for coating GPFs that operate on GDI engines. Nevertheless, these and other related studies were approached by conducting soot combustion tests (TPR or isothermal reactions) under a continuous 1 %O_2 v/v flow gas. Even though the authors of these references claim that this mode of operation roughly simulates the working conditions of a cGPF [15–17,22], the real measurements [9] confirm that oxygen concentration both in city and highway driving with a DI gasoline engine-powered passenger car is characterised always by a transient nature. Meanwhile the city driving is characterised by frequent short fuel cuts and temperatures that exceed those of diesel engines under similar driving profiles, but which are still well below what would be considered high enough for appreciable soot oxidation in diesel systems, the highway driving shows higher temperatures (that could be considered quite stable, around 500 °C), but less frequent and often fairly short fuel cuts [9]. Taking this scenario into account, a continuous flow of 1 % O_2 v/v would simulate (only very roughly) a very small O_2 concentration, which can be considered typical to those

governed by the lambda control [26,27] and not a real and representative situation of whatever mode of driving vehicle operation, characterised by O_2 pulses with different frequency in terms of the mode of driving as explained above.

To the best of our knowledge, the soot combustion reaction in GDI exhaust conditions, investigating the oxidation activity during very short O_2 pulses followed by long periods under inert atmosphere has not been previously reported in the literature. This mode of operation would represent more accurately the common conditions in GDI exhaust [9]. Even though the type of gas atmosphere chosen during the reactive pulse (only pure $^{18}O_2$) represents an idealised situation if compared with the mixture of all the real exhaust components (O_2, CO_2, H_2O….) always present in the gas stream (both during the fuel cuts and during the normal stoichiometric operation mode), an initial study which covered such a real and complex composition would be extremely difficult to be accomplished since several sources of unlabelled oxygen would be present during the long inert steps and the labelled pulse, making complex the interpretation of the catalysed soot combustion results at this initial step. The influence of CO_2 and H_2O on the performance of the catalysts, under these particular conditions, will be examined in a second stage of this study, once proved and "screened" the ability of the catalysts selected to oxidise soot under these demanding conditions.

For the detailed and congruent study of the ability showed by the catalysts selected to interact with O_2, the experiments were conducted firstly with the bare catalysts by using isotopic oxygen pulses ($^{18}O_2$) and afterwards, with the soot/catalyst mixtures under loose contact mode, which can be considered representative of the situation existing in a real coated GPF [28]. For this purpose, both three model catalysts (a pure ceria, a pure praseodymia and a home-made Pt-based catalyst, with typical composition of DPNR application) along with two sets of ceria-praseodymia mixed oxides were selected, in an attempt to investigate their ability to interact with oxygen, uptaking/releasing/exchanging with their own lattice oxygen, under several temperatures in a broad range of values. For this purpose, several Ce/Pr compositions prepared by the two different routes of preparation and exhaustively characterised in a previous publication [14], along with the model catalysts, thus conforming a high number of samples, were chosen to explore their responses under consecutive isotopic $^{18}O_2$ pulses. The final goal is to establish relationships among the physico-chemical properties of the catalysts, their capacities to activate and interact with oxygen and their soot combustion activities, at 500 ºC, under $^{18}O_2$ pulses separated by longer periods under inert atmosphere, in an attempt to emulate the situation found during highway driving with a DI gasoline engine-powered passenger car.

2. Materials and methods

2.1. Catalyst preparation

Two sets of ceria-praseodymia mixed oxides, ranging a wide range of compositions ($Ce_{1-x}Pr_xO_2$, x = 0.4, 0.6, 0.8, 1) were prepared following two simple procedures. The first one is a classic co-precipitation method, using $Ce(NO_3)_3·6H_2O$ (supplied by Aldrich, 99 %) and $Pr(NO_3)_3·6H_2O$ (supplied by Sigma Aldrich, 99.9 %) as precursors. The required amounts of each precursor were dissolved in water under mild stirring conditions. Upon complete dissolution, ammonia was added drop wise until the precipitation was complete (pH~9). The accumulated mixed oxide/hydroxide solid was recovered by filtration. It was then dried in an oven at 110 °C for 24 h, and subsequently calcined at 500 °C for 1 h in static air.

The second preparation method consisted of the direct calcination of the nitrate precursors. For this purpose, the required amounts of every precursor (in order to reach the different Ce/Pr molar compositions in the mixed oxides obtained) were intimately mixed in a mortar and subsequently calcined at 500 °C for 1 h in static air as well. The nomenclature of the samples includes the molar composition of the

mixed oxide ($Ce_{1-x}Pr_xO_2$) followed by "CP" which refers to the method of Co-Precipitation or "DC" which refers to the method of Direct Calcination of the nitrate precursors. It is important to remark that the chosen designation of the samples is only referred to their molar compositions and not to the phases and/or real compositions of the oxides obtained. More detailed information about these issues can be found elsewhere [14].

Three so-called model catalysts were selected to provide reliable and initial benchmarks. A pure CeO_2 (57 m^2/g), together with pure PrO_2 (28 m^2/g), both prepared by precipitation method using its corresponding nitrate precursor ($Ce(NO_3)_3\cdot6H_2O$ or $Pr(NO_3)_3\cdot6H_2O$) were initially chosen to provide ideas about the influence of the nature of the cation (Ce versus Pr). Additionally, a model home-made DPNR (Diesel Particulate NOx Reduction) catalyst, Pt-Ba-K/γ-Al_2O_3, with 118 m^2/g, was prepared by wetness impregnation of the support with the corresponding precursors to obtain 1.9, 11.5 and 1.4 wt% of Pt, Ba and K, respectively. The detailed procedure can be found in previous works [29,30].

2.2. Experiments with labelled oxygen

The experimental setup used to perform pulse experiments mainly consisted of a set of mass flow controllers (0.1 mL/min sensitivity), an injection valve with a 100-µL loop, and two high sensitivity pressure transducers, which allow the gas injections to be performed without concomitant pressure variation in the system. A vacuum pump was used to evacuate the helium into the loop and, once it was empty, a pressure regulator was used to fill up the loop with the isotopic gas at 8.5 psi ($2.37\cdot10^{-6}$ mol of $^{18}O_2$). The gas composition was monitored with a Pfeiffer Vacuum mass spectrometer (model OmniStar) operating at 1 s frequency. The experiments were carried out in a 5-mm inner diameter cylindrical fixed-bed reactor with 100 mg of catalyst, diluted with 180 mg SiC and packed between plugs of quartz wool. The carrier gas used was an 8 mL/min flow of He. Previously, the catalysts were treated under He at 500 °C (the temperature of catalysts' preparation) for 60 min, in an attempt to simulate a long period of non-oxidant atmosphere (stoichiometric conditions under GDI operation) [9]. After cooling down at the first temperature of reaction (200 ºC), two pulses of $2.37\cdot10^{-6}$ mol of $^{18}O_2$ were injected. The second pulse was fed once all signals reached the steady state after the first pulse. This procedure is also convenient to simulate a long period under inert atmosphere which follows a fuel cut (represented by the $^{18}O_2$ pulse). Once all MS signals reached a constant level after the second pulse, the temperature was increased in 50 °C and stabilised, and two pulses were fed at the new temperature; this procedure was repeated until the maximum temperature selected was achieved (500 ºC). Typically, minor differences were noticed between the two pulses performed at the same temperature, and the results included in the figures (that represent percentages of isotopologues) correspond to the average value obtained at each temperature. More information about this experimental set-up and its conditions of use were reported elsewhere [31] and in the Supplementary Information.
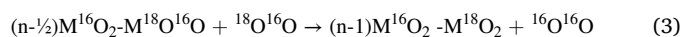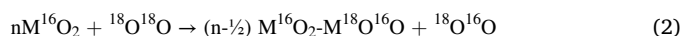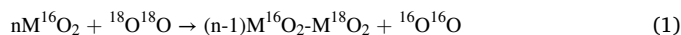
The same experiments were repeated with model soot (5 mg) and catalyst + soot mixtures (5 mg of soot + 100 mg of catalyst) by using a 1:20 soot/catalyst ratio and the so-called loose contact mode (procedure of very gentle mixture among soot and catalyst) but using only 500 °C as representative reaction temperature (which can be considered a very typical temperature in highway driving mode [9]). The model soot was supplied by Evonik-Degussa (Printex-U).

3. Results and discussion

3.1. Pulses of $^{18}O_2$ over the three model selected catalysts

In order to analyse first the nature and degree of interaction between gas phase $^{18}O_2$ and selected fresh catalysts (in other words, the capability of activating oxygen molecules over the different samples), three representative model catalysts were chosen: a pure ceria (CeO_2-CP), a

pure praseodymia (PrO_2-CP) and a home-made DPNR Pt-based catalyst (PtKBa). The responses of all the species leaving the catalytic reactor after two consecutive pulses of labelled oxygen ($^{18}O_2$) at the selected temperatures (200–500 °C) are shown in Fig. 1. The profile of an identical $^{18}O_2$ pulse over an inert SiC sample (represented in the Fig. 1a-f by a black dotted line) was taken as a reference to monitor the fast response of the gases along a solid bed with identical mass than that of the catalytic bed, but without interaction with the reactive pulse. By comparing the pattern and quantification of the $^{18}O_2$ first pulse (over SiC) with the corresponding solid lines at every temperature (200–500 °C), the response of the catalysts towards O_2 activation/consumption can be measured. At a first sight, different extents and types of interaction can be noted along the stepwise experiments, depending on the temperature and, importantly, on the nature of the catalyst. At such a low temperature as 250 ºC, part of the $^{18}O_2$ pulse already "activates" pure praseodymia and, clearly, oxygen from the lattice (^{16}O) releases as $^{16}O_2$ and $^{18}O^{16}O$ [32]. For these two types of molecules released, ^{16}O atoms come from praseodymia (or ceria), that is, there was an exchange of oxygen between the gas phase $^{18}O^{18}O$ molecules and oxygen of the metal oxide. From these experiments, the following general reactions are proposed:

$$nM^{16}O_2 + {}^{18}O^{18}O \rightarrow (n-1)M^{16}O_2\text{-}M^{18}O_2 + {}^{16}O^{16}O \tag{1}$$

$$nM^{16}O_2 + {}^{18}O^{18}O \rightarrow (n\text{-}\tfrac{1}{2})\,M^{16}O_2\text{-}M^{18}O^{16}O + {}^{18}O^{16}O \tag{2}$$

$$(n\text{-}\tfrac{1}{2})M^{16}O_2\text{-}M^{18}O^{16}O + {}^{18}O^{16}O \rightarrow (n-1)M^{16}O_2\text{ -}M^{18}O_2 + {}^{16}O^{16}O \tag{3}$$

being M = Pr or Ce.

where "n" indicates the number of $M^{16}O_2$ entities, being much higher than 1.

According to step 1, both ^{18}O atoms of the $^{18}O^{18}O$ molecules pulsed can be captured by PrO_2 (or CeO_2) and two oxygen atoms from the solid yield a $^{16}O^{16}O$ molecule. Step 2 describes the exchange of one oxygen of the $^{18}O^{18}O$ molecule by one oxygen of the oxide and, as described by step 3, these scrambled $^{18}O^{16}O$ molecules could be re-adsorbed and the remaining ^{18}O atom can be also exchanged, therefore yielding $^{16}O^{16}O$. These reactions were also identified in previous studies performed in a TAP reactor with a very low surface area ceria (2 m^2/g) [33].

Attention should be paid also to the magnitude of the different oxygen species evolved and to the shape of the species profiles. It is interesting to remark the fast response in the emission of $^{16}O_2$ for pure ceria at 500 °C after the two $^{18}O_2$ pulses (symmetrical peaks in green colour nearly coincident with the corresponding $^{18}O_2$ profile pulsed over SiC, see Fig. 1a-b) corroborating the absence of diffusional or other response's problems. Conversely, pure praseodymia presents quite asymmetrical patterns, whose starting values match with that of the "blank" experiment, but with long tails (even at the highest temperatures), thus indicating that even though the emission of exchange products begins almost concurrently when the isotopic gas is pulsed, this emission can be extended during the inert period, once the pulse becomes well finished.

Fig. 2 displays the percentages of oxygen isotopologues in the gas phase at the exit of the reactor measured at the different temperatures. Average values obtained after the two pulses, at a given temperature, were taken for the evaluation of the response of the catalysts. These values were calculated by confronting the integration of the obtained data for every oxygen species, with respect to the $^{18}O_2$ whole area of the isotopic pulses over the SiC sample (detailed information about the calculations conducted to obtain the distribution of oxygen species as well as the premises assumed for these estimations are included in SI). Different profiles are seen comparing the three catalysts selected, indicating the relevant influence of the chemical nature of the catalyst on its interaction with oxygen, as anticipated. Nevertheless, all of them are characterised by a common feature: as soon as the $^{18}O_2$ pulse is fed to the reactor, its level decreases from the starting temperature on. Considering firstly the PtKBa catalyst, shown in Fig. 2c, the decrease in the percentage of $^{18}O_2$ with increasing temperature is balanced by the increase of the $^{18}O^{16}O$ species (the predominant isotopologue up to
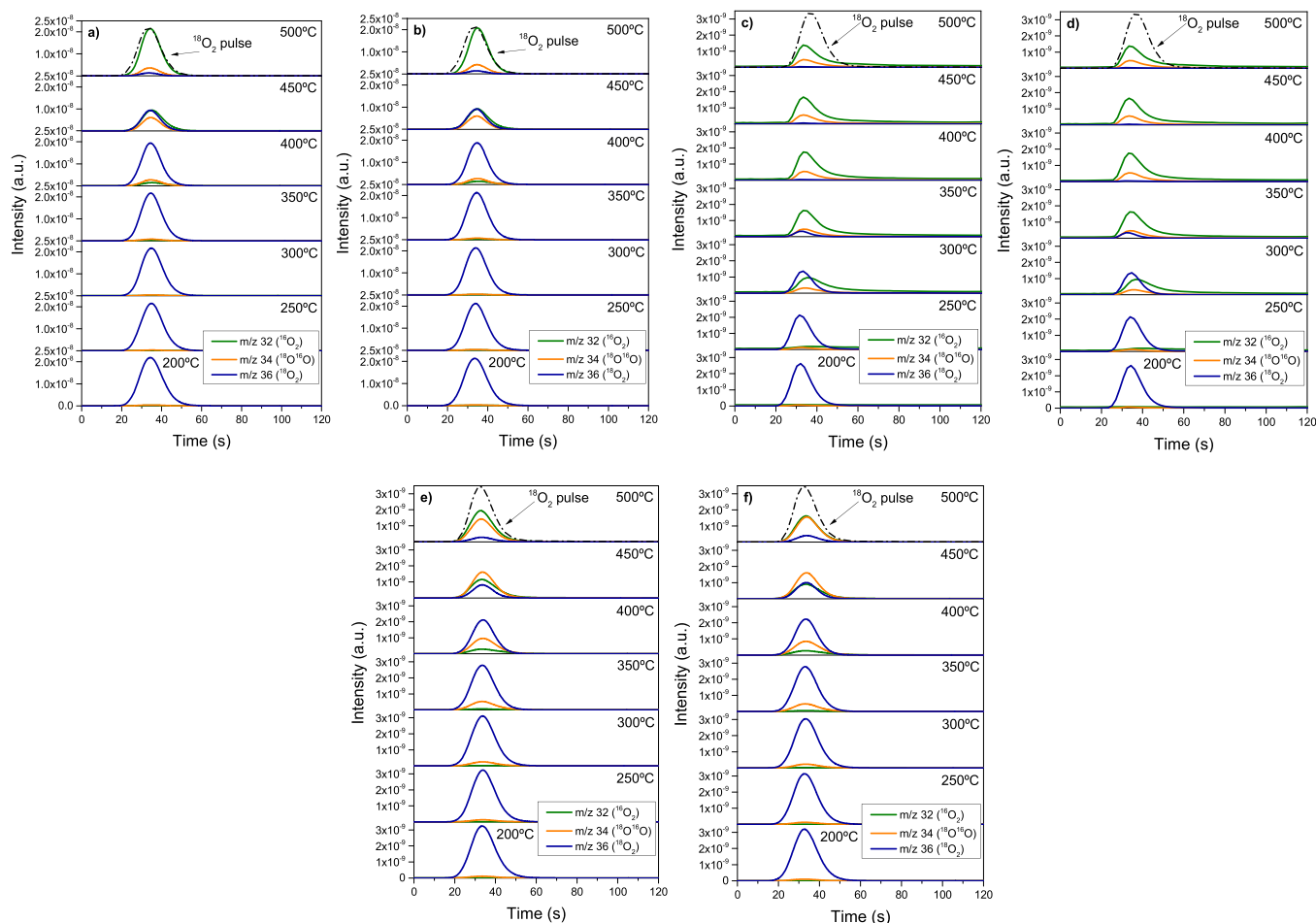
Fig. 1. Comparison of the nature of the oxygen species evolved upon $^{18}O_2$ interaction during the first pulse and the second pulse, respectively: for a pure ceria (CeO$_2$-CP) a) and b); for a pure praseodymia (PrO$_2$-CP) c) and d); and for the home-made DPNR Pt-based catalyst (PtKBa) e) and f).
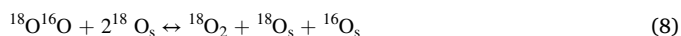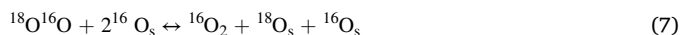
450 °C) and $^{16}O_2$. Therefore, no significant oxygen uptake is registered along the whole experiment as indicated by the black line, and, exclusively, isotopic oxygen exchange is taking place for the Pt-containing catalyst.

The basic theory of isotopic exchange considers two kinetically resolvable types of isotopic exchange, (excluding the zero-atom exchange which takes place at very low temperatures), [34–36], namely:

1. single-atom exchange between one oxygen atom from the gas phase oxygen molecule and one oxygen atom from the solid. It involves surface (or subsurface atoms of the solid), O$_s$, and may be presented as follows:

$$^{18}O_2 + {}^{16}O_s \leftrightarrow {}^{18}O^{16}O + {}^{18}O_s \qquad (4)$$

$$^{18}O^{16}O + {}^{16}O_s \leftrightarrow {}^{16}O_2 + {}^{18}O_s \qquad (5)$$

2. two-atom exchange between molecule O$_2$ and two oxygen atoms from the solid:

$$^{18}O_2 + 2{}^{16}O_s \leftrightarrow {}^{16}O_2 + 2{}^{18}O_s \qquad (6)$$

$$^{18}O^{16}O + 2{}^{16}O_s \leftrightarrow {}^{16}O_2 + {}^{18}O_s + {}^{16}O_s \qquad (7)$$

$$^{18}O^{16}O + 2{}^{18}O_s \leftrightarrow {}^{18}O_2 + {}^{18}O_s + {}^{16}O_s \qquad (8)$$

Generally speaking, simple and multiple heteroexchange mechanisms can be differentiated at the beginning of the reactions by prior appearance of $^{18}O^{16}O$ or $^{16}O_2$ in the gas phase, respectively. Since the

predominant product for the PtKBa catalyst is $^{18}O^{16}O$, the isotopic exchange seems to proceed (at least at the lowest temperatures) by a single atom-exchange type.

Conversely, the profiles exhibited by the two bare oxides are quite different compared with that of the Pt-based catalyst and among each other as well. Therefore, all these different behaviours can be considered as a *fingerprint* for the relative rate of oxygen incorporation versus oxygen dissociation and evolution of products [37]. For the bare ceria catalyst (Fig. 2a), a minor O$_2$ uptake percentage can be measured from the 250–450 °C (obtained as explained in SI). Since a small population of in situ oxygen vacancies is likely to be formed during the pre-treatment under inert atmosphere (see additional justifications in SI, Fig. S2), this could lead to a low "net" oxygen uptake to fill in these "fresh" oxygen vacancies generated. Even though, the catalysts' response might seem to be sensitive to the type of pre-treatment conducted when the estimations of percentages are normalised on the basis of oxygen uptake, (as depicted for pure ceria as a representative catalyst in Fig. S3), very similar profiles of all the oxygen isotopic species are obtained (at least for pure ceria). This confirms the validity of the trends beyond the specific pre-treatment chosen to condition the samples.

A notable feature seen from Fig. 2a (the ceria catalyst) is the occurrence of a clear maximum point in the temperature dependence of the $^{18}O^{16}O$ isotopic species (this feature was also reported for other mixed oxides [37,38]). This observation can be tentatively accounted for the two-step exchange mechanism [39]. As more and more $^{18}O^{16}O$ evolves, this interacts with the catalyst's oxygen, yielding $^{16}O_2$, since immediately after the appearance of the maximum, $^{16}O_2$ level also increases. Whatever the reaction temperature tested, the $^{16}O_2/^{18}O^{16}O$

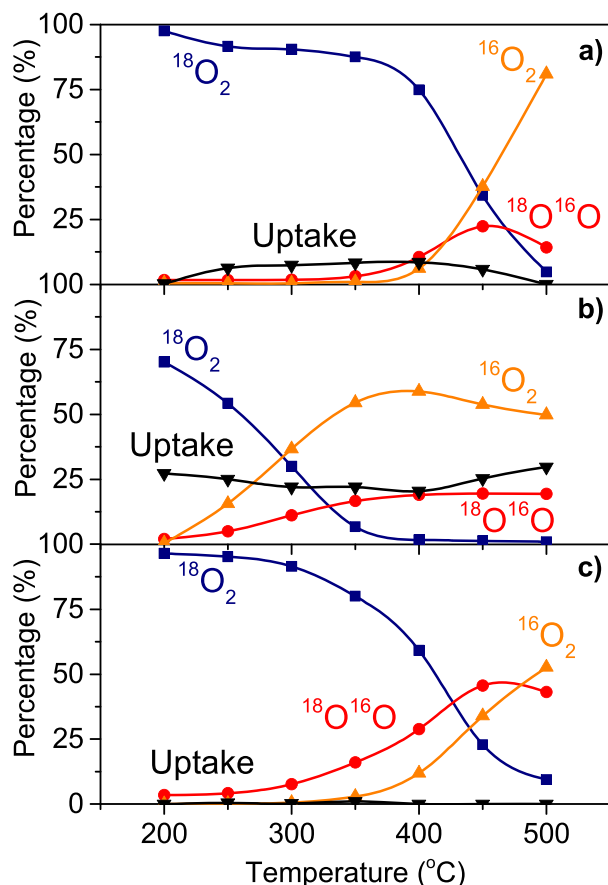**Fig. 2.** Distribution of the different oxygen species evolved upon $^{18}O_2$ interaction with: a) CeO_2-CP; b) PrO_2-CP; and c) PtKBa.

ratio remains very high, suggesting that the predominant mechanism is the two-atom exchange as usual in transition metal oxides and mixed oxides. Besides, the fact that the rate of oxygen incorporation is higher than that of oxygen dissociation could be inferred here (see corresponding black line) [37].

Concerning PrO_2-CP, this sample interacts with the $^{18}O_2$ isotopic pulse in a more dramatic way, and the kinetics of this interaction are faster, (e.g., the consumption of the pulse begins at the initial temperature −30 % of initial value- and is nearly complete at 400 °C). All the profiles are also different if compared with those of pure ceria since a relevant oxygen uptake is monitored along the experiments. This large capability of praseodymia to incorporate oxygen can be partially explained by their ability to evolve oxygen, even under inert atmosphere, if compared to pure ceria [14] (see Fig. S2 in the Supplementary Information and corresponding theoretical justifications). It is supposed that the "fresh" oxygen vacancies on praseodymia, (created during the step of heating under helium up to 500 °C), can act as "sink" centres for high levels of oxygen uptake. This would cause a remarkable interaction with oxygen (drop of the pulse) and a relevant percentage of oxygen incorporation. This would suggest that the rate of oxygen incorporation is much higher than that of oxygen release as well.

This property of releasing high amounts of oxygen under inert atmosphere (Fig. S2) is suggested to be determinant to explain the uptake's capacity attributed to pure praseodymia with regard to other physico-chemical features (such as BET surface area). Actually, this catalyst presents the lowest value of this set of samples (28 m²/g) versus ceria and the Pt-based catalyst (which present 57 m²/g and 118 m²/g, respectively).

PrO_2-CP also presents a much faster response towards $^{16}O_2$ emission at low temperatures. Referenced literature [40] reports that both simple

and multiple heteroexchange occur for mixed oxides. Nevertheless, as demonstrated for the case of $Ce_xZr_{1-x}O_2$ mixed oxides [40], multiple heteroexchange seems to be much more dominant for pure praseodymia at the very beginning of the experiment with regard to pure ceria. Multiple heteroexchange occurs with simultaneous participation of two oxygen atoms of the oxide. Surface dioxygen intermediates involved could be superoxides (O_2^-) or peroxides (O_2^{2-}) as proposed by several authors [41–43]. It could be tentatively suggested that this catalyst presents a tremendous ability to capture $^{18}O_2$, as measured, but also to exchange $^{18}O_2$ with the remaining O_2^{2-} (peroxo) and O_2^- (superoxo) groups on the catalyst surface since $^{16}O_2$ seems to prevail since 250 °C, differently to the trends in emission products shown by the Pt-containing catalyst and CeO_2.

As more and more $^{18}O_2$ is uptaken by PrO_2-CP, even though $^{16}O_2$ keeps being the prevalent species, both $^{16}O_2$ and $^{18}O^{16}O$ levels tend to converge at the highest temperatures (Fig. 2b). Therefore, for PrO_2-CP, the interaction with oxygen is dominated by the incorporation of the $^{18}O_2$ pulse and the evolution of products is conditioned by the level of oxygen uptaken, as the experiment progresses. Even considering this, the emergence of $^{18}O_2$ as reaction product is not observed in the final steps of the experiment, thus excluding completely the occurrence of the last step of the two-atom exchange type.

Repeated tests were conducted over this pure praseodymia oxide to verify the reproducibility of the oxygen uptake extension. Good repeatability was found, and the detailed profiles are compiled on SI (Fig. S4).

3.2. Pulses of $^{18}O_2$ over the ceria-praseodymia mixed oxides

Due to the very different and positive behaviour of pure praseodymia versus pure ceria, the impact of the Ce/Pr composition (ranging the whole range of formulations) as well as the type of preparation method on the response of all the mixed oxides prepared will be analysed in this section. Fig. 3 and Fig. 4 depict the same information than that displayed in Fig. 2 but for the sets of $Ce_{1-x}Pr_xO_2$ catalysts (with x ranging from 1 to 0.4), for those samples prepared by the direct calcination method (Fig. 3) and by the co-precipitation method (Fig. 4), respectively.

Generally speaking, all the Pr-based catalysts highly interact with the $^{18}O_2$ pulses, thus improving the response of the Pt-containing catalyst and, more importantly, that of the ceria catalyst, despite of their lower surface areas.

Additionally, remarkable differences are revealed by using one or other method of preparation. In fact, whatever the composition chosen, the catalysts prepared by co-precipitation (Fig. 4) seem to interact with the $^{18}O_2$ pulses at lower temperatures and in higher extents than their counterparts prepared by the direct calcination method (Fig. 3), and the same applies for the $^{18}O_2$ uptake capacity. This is directly represented in a more visual and effective way in Fig. S5 (a-d) of the Supplementary Information. The profiles are obviously affected by the Ce/Pr ratio, in other words, there are differences in every series depending on the Pr content of the oxides, but this cannot be systematised and explained in an easy way due to the fact that the BET surface area does not exhibit the same trends or variations in terms of the Pr content of the mixed oxides along the two sets of catalysts studied. Regarding the emission of exchange products, it can be said that, in general: i) DC-catalysts exchange more O_2 with the molecules of the isotopic pulses, yielding more $^{16}O_2$, whatever the composition tested; ii) the corresponding yields of the scrambled product ($^{18}O^{16}O$) are quite similar among them for all the compositions of the series (with the exception of PrO_2-DC, which presents a very low BET surface area); and iii) the corresponding yields of CP-catalysts (both $^{18}O^{16}O$, but mainly $^{16}O_2$), are, in general, lower than their counterparts of DC-series.

By a detailed inspection and comparison of all the representations of Figs. 3 and 4, one can see high $^{18}O_2$ consumptions at the beginning of the experiments accompanied by very high oxygen uptakes capacities for all the oxides of the CP-series. Conversely, low $^{18}O_2$ pulse consumptions
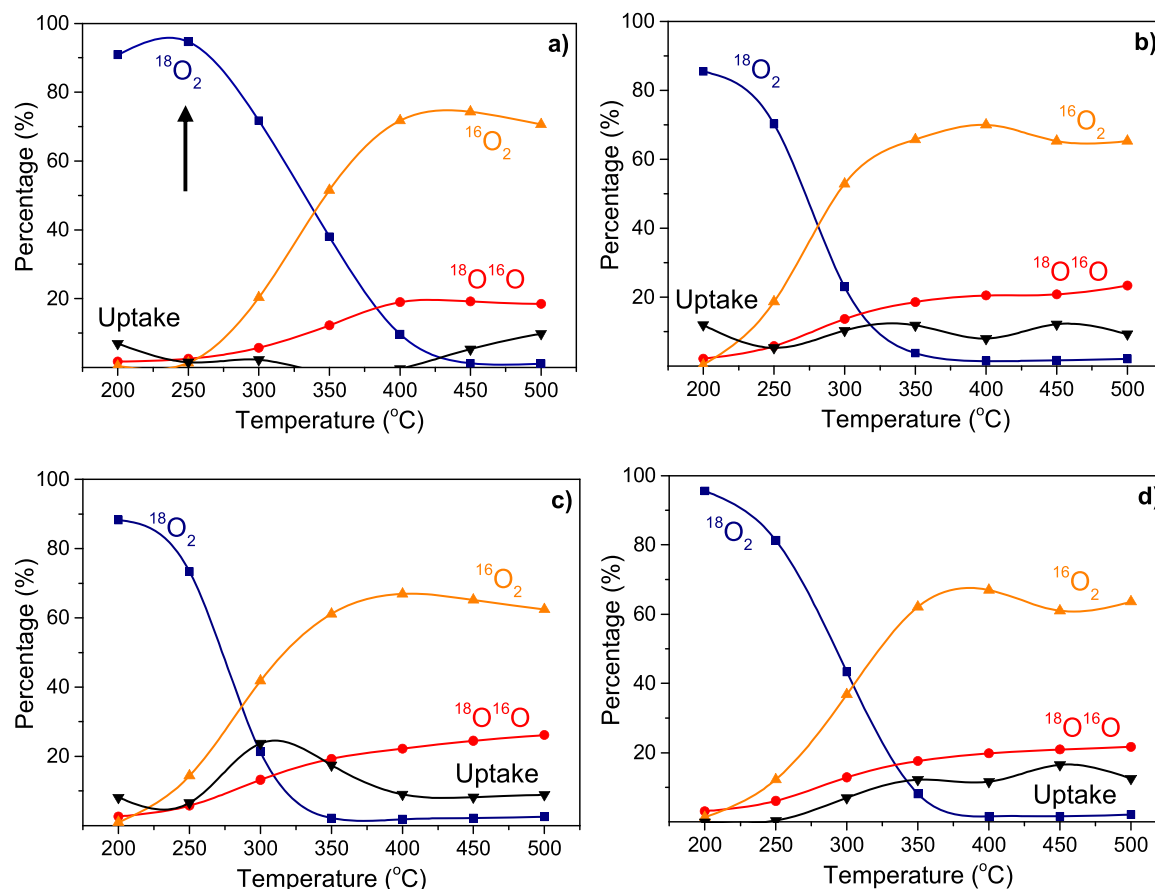
Fig. 3. Gas phase distribution of different oxygen isotopologues ($^{16}O_2$, $^{18}O^{16}O$ and $^{18}O_2$) and oxygen uptake with respect to the inlet labelled oxygen at different temperatures under He flow over a) PrO_2-DC, b) $Ce_{0.2}Pr_{0.8}O_2$-DC, c) $Ce_{0.4}Pr_{0.6}O_2$-DC and d) $Ce_{0.6}Pr_{0.4}O_2$-DC.

along with low values of $^{18}O_2$ uptake characterise to the DC-series' catalysts, at the lowest temperatures. This leads us to confirm that regardless of the differences in BET surface areas which make difficult a systematic comparison among methods/compositions, it is clear that different methods used yield to different initial features on the surface/subsurface of the catalysts that lead to crucial differences and influence on the oxygen interaction capacity of the catalysts. However, as soon as the experiment progresses and more and more $^{18}O_2$ molecules are pulsed onto the catalysts, the kinetics of $^{18}O_2$ consumptions become different and some of the samples practically consume all the $^{18}O_2$ pulses at 350 °C, meanwhile other catalysts do not completely consume the pulses even at 500 ºC.

In order to shed some light on this issue, some calculations were estimated with the purpose to obtain information about the specific number of $^{18}O_2$ pulses to reach an amount of ^{18}O equal to that of the surface oxygen atoms onto the several catalysts, since they present a wide range of BET surface areas (from 6 to 47 m²/g). The number of surface oxygen atoms for every catalyst may be calculated from the BET surface area, assuming similar structures and taking the value given by Madier et al. [40] (13.7 atoms·nm², for ceria-based oxides). Table 1 lists some relevant information useful to interpret the profiles, extends and rates of O_2 pulse consumptions that make a difference among the catalysts. In this sense, not only the number of oxygen pulses needed to exchange/saturate the whole surface of every catalyst was calculated (according to the O atoms that contain the number of $^{18}O_2$ pulses injected), as compiled on Table 1, but also the number of oxygen pulses needed to exchange the whole oxygen atoms considering also the bulk level (245 pulses). Assuming the general premise that all the oxygen linked to cerium or praseodymium atoms are equally susceptible to participate in the uptake/exchange processes, the wide dispersion of

BET surface areas of the catalysts leads to the fact that after the whole experiment, (14 $^{18}O_2$ pulses), some samples have readily suffered the "saturation" of their surfaces and others not. This is intended to be depicted on Figs. 3 and 4 by a vertical black arrow, indicating the temperature at which the number of O atoms from the pulses injected have eventually matched with the oxygen surface atoms initially exposed on every catalyst. Accordingly, the samples with the lowest BET surface areas (PrO_2-DC, $Ce_{0.2}Pr_{0.8}O_2$-CP y $Ce_{0.4}Pr_{0.6}O_2$-CP) suffer saturation of their surface oxygen numbers at low temperatures in the course of the whole experiment. Therefore, subsurface/bulk oxygen participation should be assumed for the mentioned catalysts at the temperatures above 250 and 300 °C, as marked with the black arrows on the Figs. 3a, 4b, 4c and 4a (in this last case just at the end of the experiment), thus allowing us to assert that this oxygen participation beyond the external oxygen layer could affect the rate of both oxygen consumption/uptake exchange, thus slowing down the interaction/consumption of the $^{18}O_2$ pulses, since subsurface/bulk oxygen mobility is affecting the processes as well, and not only the participation of exposed surface oxygens. Actually, $^{18}O_2$ could be emerging as new product of oxygen exchange (not discernible from the $^{18}O_2$ fraction that does not interact with the catalyst). To support these asseverations, the following example is provided: $Ce_{0.2}Pr_{0.8}O_2$-CP and $Ce_{0.4}Pr_{0.6}O_2$-CP do not reach 100 % values of $^{18}O_2$ consumptions even at 450 °C and present the lowest slopes on their representations). Since it is reasonable to assert that for participation of oxygen coming from subsurface layers, bulk oxygen diffusion becomes an important parameter to take into account and, in principle, this participation would be more hindered than that of the surface oxygens. All these ideas could, at least, partially explain, the differences in the profiles beyond the method employed and the Ce/Pr composition used. Accordingly, samples that do not suffer "saturation" in the number of
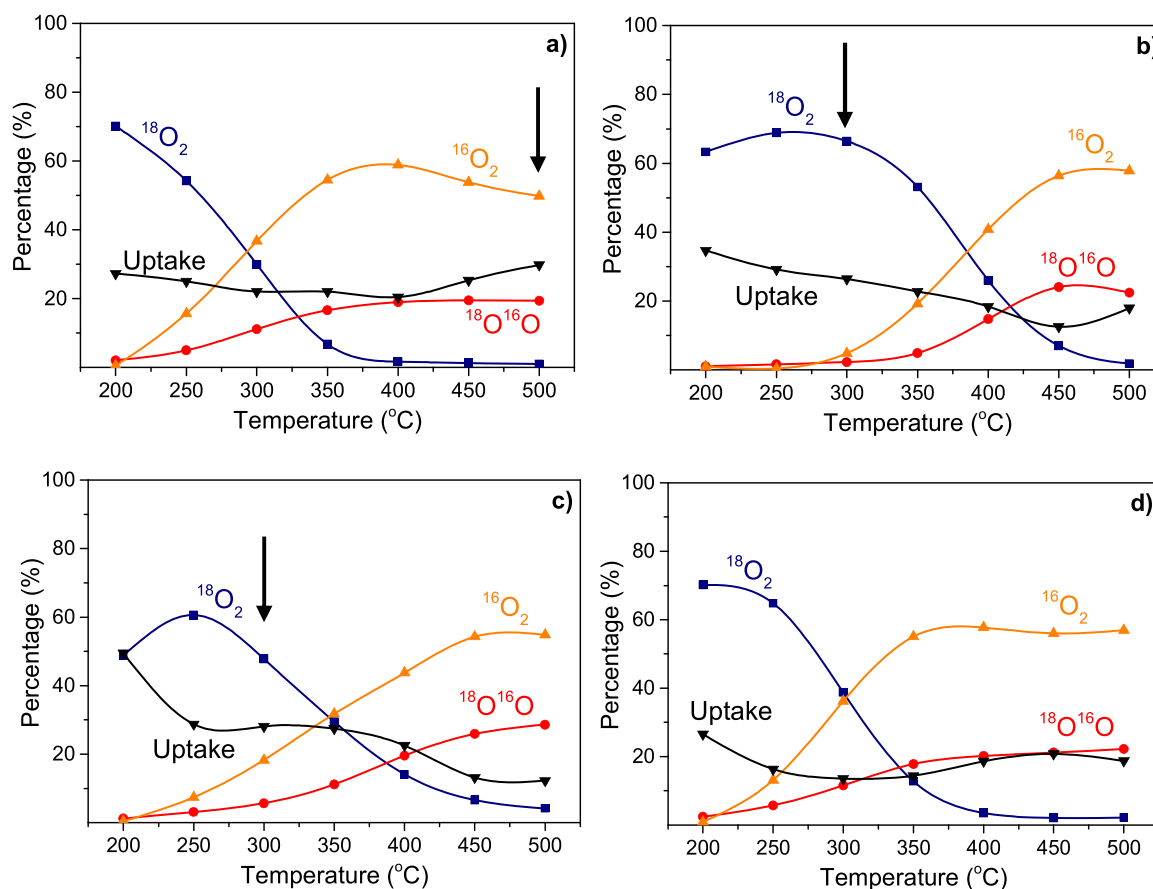
Fig. 4. Gas phase distribution of different oxygen isotopologues ($^{16}O_2$, $^{18}O^{16}O$ and $^{18}O_2$) and oxygen uptake with respect to the inlet labelled oxygen at different temperatures under He flow over a) PrO_2-CP, b) $Ce_{0.2}Pr_{0.8}O_2$-CP, c) $Ce_{0.4}Pr_{0.6}O_2$-CP and d) $Ce_{0.6}Pr_{0.4}O_2$-CP.

Table 1
Number of $^{18}O_2$ pulses needed to saturate the Ce-Pr catalysts at surface level.

Catalyst	S_{BET} (m²/g)	Number of pulses to saturate the surface
PrO_2-CP	28	13
$Ce_{0.2}Pr_{0.8}O_2$-CP	10	4
$Ce_{0.4}Pr_{0.6}O_2$-CP	11	5
$Ce_{0.6}Pr_{0.4}O_2$-CP	38	18
PrO_2-DC	6	3
$Ce_{0.2}Pr_{0.8}O_2$-DC	31	14
$Ce_{0.4}Pr_{0.6}O_2$-DC	47	22
$Ce_{0.6}Pr_{0.4}O_2$-DC	40	19

* The number of pulses to saturate the bulk solids is 245.

surface oxygen atoms due to their higher BET surface areas, are characterised by fast kinetics of $^{18}O_2$ pulses consumptions, independently on the initial value of $^{18}O_2$ consumption (%) and the preparation method, reaching 100 % of $^{18}O_2$ consumption values (in other words, 0 % of emission value) since medium temperatures until the end of experiment (e.g. $Ce_{0.4}Pr_{0.6}O_2$-DC with 47 m²/g, at 350 °C). Therefore, the involvement of external surface area and subsequent participation of subsurface layers might play an important role on the oxygen interaction process with the catalysts for the Pr-containing oxides investigated. For pure ceria (without Pr incorporation in the formulation), these ideas do not apply, since all the profiles and activities measured allow us to assert that the level of interaction and activation with O_2 is lower (there is no whole $^{18}O_2$ consumption at 500 °C, low levels of O_2 uptake are detected and the capacity of oxygen exchange is displaced at higher temperatures).

By selecting a temperature of 400 °C (as a temperature at which

oxygen exchange products levels seem to be apparently stabilised) and collecting the four parameters under study for the whole catalysts investigated (shown in Table 2), interesting guidelines can be deduced:

i) Pr-containing samples are much more active concerning activation and interaction with the $^{18}O_2$ pulses than pure ceria, despite of their lower BET surface areas. This is connected with their very high reducibility under inert atmosphere, as further explained by combining characterisation measurement data in SI (Table S2).

ii) The co-precipitated samples (whatever the BET surface area that possess) are characterised by high levels of $^{18}O_2$ consumption at the beginning of the experiments and high levels of oxygen uptake if compared with those of the direct-calcination catalysts.

iii) Congruently with those experimental observations, DC-samples, which are characterised by lower capacities of oxygen uptake, exchange more oxygen than the corresponding CP-samples, thus yielding to higher percentages of $^{16}O_2$, slightly higher of $^{18}O^{16}O$ and higher ratios of $^{16}O_2/^{18}O^{16}O$, than those of CP-samples.

iv) The kinetics of fast O_2 interaction and consumption in terms of temperature are highly influenced by the BET surface area, (much more than by the method of preparation and the Ce/Pr ratio), as seen in Figs. 3 and 4.

In order to stablish some reliable comparisons among the two methods, since the BET surface area has been revealed as an important parameter, (in connection with the kinetics of O_2 pulses consumption during the whole experiment), attention will be paid now to the possible influence of the route of preparation on the catalytic behavior. For this purpose, $Ce_{0.6}Pr_{0.4}O_2$-DC and $Ce_{0.6}Pr_{0.4}O_2$-CP were selected since they present very similar BET surface area (40 and 38 m²/g, respectively),

Table 2

Gas phase distribution of the different oxygen isotopologues ($^{18}O_2$, $^{18}O^{16}O$ and $^{16}O_2$) and oxygen uptake for the catalysts at 400 ºC after injecting the $^{18}O_2$ pulse.

Catalyst	$^{18}O_2$ (%)	$^{18}O^{16}O$ (%)	$^{16}O_2$ (%)	Oxygen uptake (%)[a]	Ratio $^{16}O_2/^{18}O^{16}O$
CeO$_2$-CP	75	11	6	8	0.5
PtKBa	59	29	12	0	0.4
PrO$_2$-CP	2	19	59	20	3.1
Ce$_{0.2}$Pr$_{0.8}$O$_2$-CP	26	15	41	18	2.7
Ce$_{0.4}$Pr$_{0.6}$O$_2$-CP	14	20	44	23	2.2
Ce$_{0.6}$Pr$_{0.4}$O$_2$-CP	4	20	58	19	2.9
PrO$_2$-DC	10	19	72	0	3.8
Ce$_{0.2}$Pr$_{0.8}$O$_2$-DC	1	20	70	8	3.5
Ce$_{0.4}$Pr$_{0.6}$O$_2$-DC	2	22	67	9	3.0
Ce$_{0.6}$Pr$_{0.4}$O$_2$-DC	2	20	67	12	3.4

[a] Oxygen uptake (%) = 100 - ($^{18}O_2$ (%) + $^{18}O^{16}O$ (%) + $^{16}O_2$ (%)).

and both share the common feature that only surface oxygen atoms are involved during the whole experiment. For this particulate case, if differences are noted between the samples, the method of preparation should be the only parameter to take into account. As already mentioned as a general guideline, Ce$_{0.6}$Pr$_{0.4}$O$_2$-CP presents a high capacity of consumption of $^{18}O_2$ pulses, at the beginning of the experiment, joined to very high oxygen uptake values, however, as the experiment proceeds, the rate of $^{18}O_2$ consumption begins to slow down. Conversely, Ce$_{0.6}$Pr$_{0.4}$O$_2$-DC is characterised by much lower values of O$_2$ consumption at the lowest temperatures along with very low O$_2$ uptakes capacities. As the experiment progresses, the whole consumption of the $^{18}O_2$ pulses is seen before for Ce$_{0.6}$Pr$_{0.4}$O$_2$-DC and, in accordance with lower oxygen uptake capacities, the percentages of oxygen exchange products ($^{18}O^{16}O$ and $^{16}O_2$) are higher, as well as the $^{16}O_2/^{18}O^{16}O$ ratio, if compared with those of Ce$_{0.6}$Pr$_{0.4}$O$_2$-CP (please see data on Table 2). Even though the whole characterisation results concerning these mixed oxides catalysts were presented elsewhere [14], some information is compiled in Table S1, revealing that a better atomic homogeneous distribution (between Ce and Pr into the lattice) can be inferred from the physico-chemical characterisation and this would tentatively be the reason of the very different behaviour under pulse conditions. In this line, the cell parameter (a) is higher for Ce$_{0.6}$Pr$_{0.4}$O$_2$-CP [14], suggesting a superior degree of cation insertion and/or higher contribution of Pr^{3+}. Higher value of the I$_{vacancies\ band}$/I$_{F2g}$ ratio corroborates a higher population of oxygen vacancies for Ce$_{0.6}$Pr$_{0.4}$O$_2$-CP as well (Table S1), which would favour more oxygen interaction, activation and uptake for Ce$_{0.6}$Pr$_{0.4}$O$_2$-CP with regard to Ce$_{0.6}$Pr$_{0.4}$O$_2$-DC. The better atomic homogeneity in terms of cerium and praseodymium distribution might be verified by confronting the XPS results (see comparison among Ce/Pr surface atomic ratios versus Ce/Pr nominal atomic ratios for these representative catalysts on Table S1).

Finally, in an attempt to find some useful correlations comprising Ce/Pr ratios, method of preparation and the parameters that reflect oxygen interaction capacity of the catalysts along with O$_2$ emission capacities during a He-TPD (discussed in a previous publication [14]), Fig. 5 depicts the attempts to illustrate some correlations representing the mentioned parameters both expressed per gram of catalyst (Fig. 5a) and per gram of square meter, (Fig. 5b); due to the fact that the variation of BET surface area against Pr content does not follow any trend for the mixed oxides obtained from CP method and an abrupt decrease is seen at high Pr contents. As depicted on Fig. 5a, the amount of O$_2$ emitted, integrated up to 500 °C (obtained from He-TPD experiments) and the "accumulated" oxygen uptake capacity up to 500 °C (integrated up to the final of the experiment, after the 14 $^{18}O_2$ pulses) appear not to follow clear trends regardless of the method of synthesis (both for co-precipitated, depicted in orange colour, and direct calcination-samples, depicted in blue). However, the values of O$_2$ emitted are quite close among identical compositions for both series (represented by dotted lines), excepting for the case of pure praseodymia, indicating that one of the main responsible of this behaviour seems to be the reducibility of the own Pr loading for every catalyst and not the method of preparation. Conversely, the parameter so-called "oxygen uptake" is quite different among the same Ce/Pr compositions, thus suggesting that the step of "refilling" with oxygen after a pre-treatment under He is a very sensitive process in terms of the method of preparation and the catalysts' features, (and not only governed by the Pr content), being always superior for CP-samples. The differences become more and more relevant if these values are expressed per square meter (BET surface area) and again represented versus Pr content (Fig. 5b). A volcano trend is exhibited by CP-series, meanwhile this trend does not appear for DC-catalysts (increasing nearly monotonically with the Pr content). These figures depict the complex interplay among the values of BET surface areas, Ce/Pr compositions and method of preparation towards the capacity of releasing and activating O$_2$
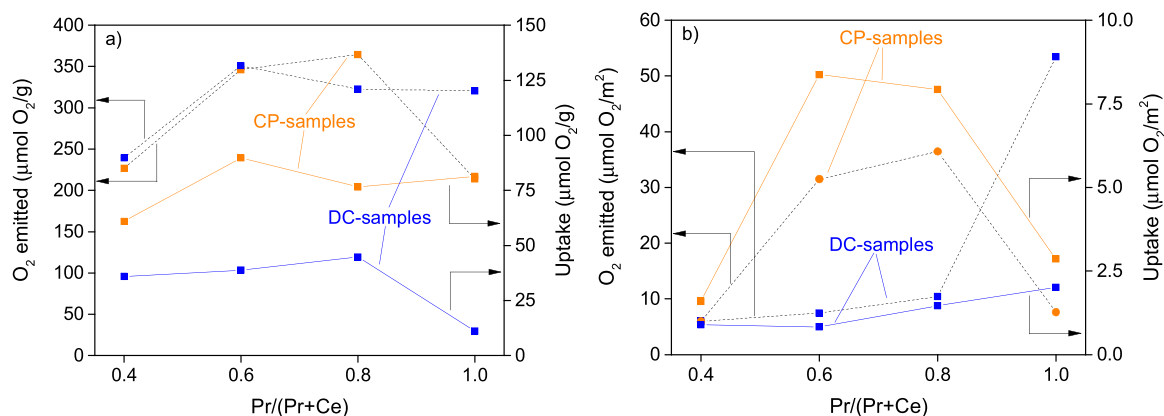

Fig. 5. Correlations of O$_2$ emitted up to 500 °C and O$_2$ uptake versus Ce/Pr ratios for the investigated catalysts normalised by: a) mass (gram of catalyst), and b) surface area (square meter of catalyst).

molecules which is suggested to be difficult to "split out" one from each other, if an attempt to rationalise the impact of every variable on the catalysts' performances is desired to be conducted.

As a brief summary, even though no conclusive correlations were found with increasing Pr content for every set of catalysts prepared, CP-catalysts, (whatever the composition considered) are more effective for incorporating oxygen from the isotopic pulses. The benefits become more and more accentuated if the parameters analysed are expressed per BET surface area, due to the "collapse" in specific area suffered by the mentioned catalysts, at high Pr contents, (CP-series), which is one of the reasons of the pattern of the representations ("volcano profile").

For all the mentioned issues, the two catalysts having the same molar composition in Ce/Pr and very similar BET surface areas ($Ce_{0.6}Pr_{0.4}O_2$-CP and $Ce_{0.6}Pr_{0.4}O_2$-DC) were chosen to conduct and discuss the results of soot combustion under pulse conditions, and thus evaluating in a more certain way the impact of the method of preparation. But firstly, and for the sake of clarity, the results derived from the uncatalysed soot combustion and those from the model catalysts will be presented in the next section (in a parallel way to the previous sections).

3.3. Soot combustion results

As a short reminder, it is interesting to note that the management of the soot accumulated within a particle filter during different driving conditions still remains an important challenge for gasoline-powered vehicles, especially GDI. In DI gasoline engine-powered passenger car, there are essentially no NO_2 and O_2 available for soot combustion under normal stoichiometric operation ($\lambda = 1$). Oxygen is only available during fuel cuts, when the engine pumps air from the intake to the exhaust, as anticipated in the introduction. Besides, both the transient exhaust temperature and oxygen concentration largely depend on the driving mode [9]. Therefore, to assess the impact of the Ce-Pr catalysts on soot combustion activity under the simulated fuel cuts, experiments of $^{18}O_2$ pulses have been carried out on the studied catalysts with Printex-U soot

at 500 °C, with long periods of time under inert gas, between the injected pulses. These chosen conditions simulate in a simplified way the temperature and very low-frequency oxygen pulses that can occur in a highway driving mode for a GDI vehicle, according to Boger et al. [9].

The uncatalysed oxidation of model soot was studied under identical conditions than those presented for the two consecutive $^{18}O_2$ pulses. Fig. 6 shows the set of the three CO_2 isotopologues profiles for the uncatalysed reaction during the second pulse (Fig. 6a, b and c, in black lines). For the sake of brevity, only the second pulse is shown in this figure. $C^{18}O_2$ is the most abundant isotopologue among the three possible ones in the uncatalysed soot combustion experiments. However, this situation is very different from that presented by the model catalysts, whose main isotopologue is $C^{16}O_2$ (as can be clearly illustrated by comparing the quantifications shown in Table 4 with those of Table 3, where all the possible products emitted were quantified in arbitrary unities for both pulses). Since the $C^{16}O_2$ emissions are several orders of magnitude higher than those of $C^{18}O^{16}O$ and $C^{18}O_2$, Fig. 6 only collects the $C^{16}O_2$ isotopologue (as majority product) for the model catalysts.

These results confirm the direct attack of $^{18}O_2$ to soot in the absence of a model catalyst [33,44,45]. The secondary isotopologue was $C^{18}O^{16}O$. Unlabelled oxygen must come from surface oxygen complexes present on the soot surface before the $^{18}O_2$ pulse. In fact, the oxygen content of the model soot Printex-U used in these experiments was estimated from elemental analysis to be around 3–4 wt% [46,47], this oxygen being the source of unlabelled oxygen. $C^{18}O$ was also detected as well and minor amounts of $C^{16}O$. Indeed, it is noteworthy that the ratio of products area $\Sigma CO_2(C^{18}O_2 + C^{18}O^{16}O + C^{18}O_2)/\Sigma CO(C^{18}O + C^{16}O)$, in Table 3, is quite similar to that obtained in uncatalysed Printex-U combustion with oxygen in a flow reactor (selectivity towards CO_2 around 60 %) [12].

For the uncatalysed reaction, the formation of $C^{18}O_2$ and $C^{18}O$ can be described as:

$$C + {}^{18}O_2 \rightarrow C^{18}O_2 \tag{9}$$

$$2\,C + {}^{18}O_2 \rightarrow 2\,C^{18}O \tag{10}$$

Conversely, for the catalysed reactions employing the model catalysts (and with the rest of the catalysts studied, that will be commented on), a very high selectivity towards $C^{16}O_2$ was monitored (and the rest of CO_2 and CO isotopologues emissions were negligible). This is the reason why the quantification has been approached only for $C^{16}O_2$. This experimental evidence suggests the strong involvement of oxygen species coming from the model catalysts in soot combustion.

When oxygen was pulsed under He, almost all the $^{18}O_2$ disappeared at 500 °C (contrary to what was observed for the uncatalysed reaction), but the presence of labelled oxygen molecules ($^{18}O_2$ and $^{18}O^{16}O$) after the pulse for CeO_2-CP and PtKBa catalysts was detected (Fig. 7). The latter phenomenon was not observed for PrO_2-CP and neither for any of the ceria-praseodymia mixed oxides. Nevertheless, $C^{16}O_2$ emerges with
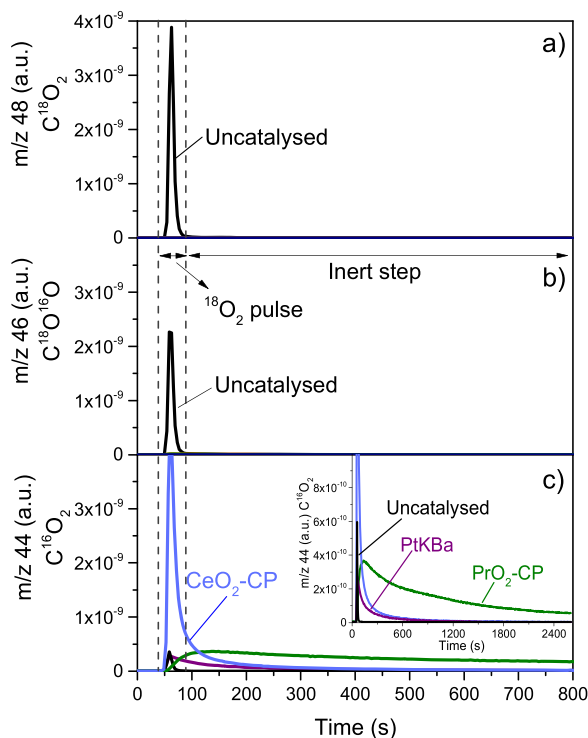

Fig. 6. CO_2 isotopologue profiles after injection of the second $^{18}O_2$ pulse over soot-catalyst loose contact mixture at 500 °C under He flow for: a) $C^{18}O_2$ isotopologue, b) $C^{18}O^{16}O$ isotopologue, and c) $C^{16}O_2$ isotopologue. The uncatalysed test has been added for comparative purposes.

Table 3
Area integration of each CO_2 and CO isotopologues MS intensities during the injection of the first and the second $^{18}O_2$ pulse for the uncatalysed soot combustion test (500 °C).

Isotopologue	Area integration of the corresponding signal obtained by MS (a.u.)	
	1st pulse	2nd pulse
$C^{18}O_2$	$6.6 \cdot 10^{-8}$	$4.3 \cdot 10^{-8}$
$C^{18}O^{16}O$	$4.7 \cdot 10^{-8}$	$2.8 \cdot 10^{-8}$
$C^{16}O_2$	$1.1 \cdot 10^{-8}$	$6.3 \cdot 10^{-9}$
$C^{18}O$	$3.4 \cdot 10^{-8}$	$2.1 \cdot 10^{-8}$
$C^{16}O$	$2.5 \cdot 10^{-8}$	$1.6 \cdot 10^{-8}$
Selectivity to CO_2 (%)[a]	67.9	68.0

[a] $\text{Selectivity to } CO_2(\%) = \dfrac{(C^{18}O_2 + C^{18}O^{16}O + C^{16}O_2)}{(C^{18}O + C^{16}O) + (C^{18}O_2 + C^{18}O^{16}O + C^{16}O_2)} \cdot 100$
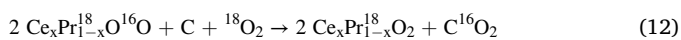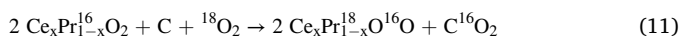
Table 4

Area integration of each CO_2 isotopologue MS intensities during the injection of the first and the second $^{18}O_2$ pulse for some of the most representative catalysts under soot combustion test (500 ºC).

CO_2 isotopologue	Pulse	Area of integration of the corresponding signal obtained by MS				
		CeO_2-CP	PtKBa	PrO_2-CP	$Ce_{0.6}Pr_{0.4}O_2$-CP	$Ce_{0.6}Pr_{0.4}O_2$-DC
$C^{18}O_2$	1st	$1.3\cdot10^{-12}$	$1.7\cdot10^{-13}$	$2.4\cdot10^{-12}$	$2.2\cdot10^{-12}$	$1.9\cdot10^{-12}$
	2nd	$1.4\cdot10^{-12}$	$0.8\cdot10^{-11}$	$3.5\cdot10^{-12}$	$6.8\cdot10^{-12}$	$2.0\cdot10^{-12}$
	Total[a]	$2.8\cdot10^{-12}$	$0.8\cdot10^{-11}$	$5.9\cdot10^{-12}$	$9.1\cdot10^{-12}$	$4.0\cdot10^{-12}$
$C^{18}O^{16}O$	1st	$2.9\cdot10^{-10}$	$2.1\cdot10^{-10}$	$1.3\cdot10^{-9}$	$6.4\cdot10^{-10}$	$4.2\cdot10^{-10}$
	2nd	$3.0\cdot10^{-10}$	$0.9\cdot10^{-9}$	$1.7\cdot10^{-9}$	$7.5\cdot10^{-10}$	$4.3\cdot10^{-10}$
	Total[a]	$5.9\cdot10^{-10}$	$1.1\cdot10^{-9}$	$3.0\cdot10^{-9}$	$1.4\cdot10^{-9}$	$8.5\cdot10^{-10}$
$C^{16}O_2$	1st	$1.1\cdot10^{-7}$	$1.0\cdot10^{-7}$	$4.6\cdot10^{-7}$	$5.0\cdot10^{-7}$	$1.5\cdot10^{-7}$
	2nd	$1.1\cdot10^{-7}$	$6.8\cdot10^{-8}$	$4.9\cdot10^{-7}$	$5.5\cdot10^{-7}$	$1.5\cdot10^{-7}$
	Total[a]	$2.2\cdot10^{-7}$	$1.8\cdot10^{-7}$	$9.5\cdot10^{-7}$	$1.0\cdot10^{-6}$	$3.0\cdot10^{-7}$

[a] Total corresponds to the sum of the values obtained from both oxygen pulses (1st and 2nd) for each catalyst.

very different profiles (Fig. 6c). As anticipated, $C^{16}O_2$ was practically the only carbon-containing product observed, evidencing that the oxygen from isotopic pulses did not react directly with soot, verifying that catalysts' oxygen was transferred to soot and $^{18}O_2$ filled up the possible vacancies created. In this regard, Bueno et al. previously observed that ceria can act as a pump in the pulse regime, supplying initially its lattice oxygen to the soot instead of the own oxygen from the pulse after injecting [33,48]. Furthermore, all these evidences are in good agreement with the generally assumed Mars-van-Krevelen mechanism for soot oxidation with ceria-based catalysts [49,50], where the active oxygen species (used for soot combustion) come from the surface-/subsurface of the oxide towards the soot particles and are initially unlabelled oxygen species, as indicated in the following general equations:

$$2\, Ce_xPr_{1-x}^{16}O_2 + C + {}^{18}O_2 \rightarrow 2\, Ce_xPr_{1-x}^{18}O^{16}O + C^{16}O_2 \quad (11)$$

$$2\, Ce_xPr_{1-x}^{18}O^{16}O + C + {}^{18}O_2 \rightarrow 2\, Ce_xPr_{1-x}^{18}O_2 + C^{16}O_2 \quad (12)$$

In the particular case of PtKBa sample, the soot combustion process takes place through the involvement of different chemical entities compared with ceria-based catalysts. Namely, the oxidation of the carbon centres from soot is restricted to the intervention of the oxygen-containing Pt-O-M centres, where "M" represents an alkaline or alkaline-earth metal (K or Ba), as reported elsewhere [30], which yields a low soot combustion activity under these experimental conditions, compared with the rest of the catalysts. Accordingly, a high $^{16}O_2$ emission is detected during the $^{18}O_2$ pulse (Fig. 7c), indicating a "scarce use" of the exchanged oxygen for the purpose of the soot combustion reaction.

Focusing on the unlabelled CO_2 emission profile, there are significant differences in the evolution of this combustion product over time (as shown in Fig. 6c). Firstly, the uncatalysed test shows a very symmetrical and narrow unlabelled CO_2 peak, which indicates just a very short-term interaction with Printex-U soot as a function of time. At a glance, the most featured peak of $C^{16}O_2$ corresponds to CeO_2-CP, as it produces a very high emission of CO_2 in a short period of time. This catalytic behaviour contrast sharply with PrO_2-CP catalyst, which presents a peak with a lower CO_2 maximum. However, although PrO_2-CP's profile does not reach such an exalted peak as that of CeO_2-CP, a significant long-term soot combustion (much higher than that of CeO_2-CP) is observed, where the $C^{16}O_2$ emission decays very slowly over time during the inert step (Fig. 6c shows the same form zoomed). In the case of PtKBa catalyst, the emission of the main $C^{16}O_2$ isotopologue compared to the other two model catalysts is clearly inferior and the tail of CO_2 emission can be considered almost negligible as well. A possible explanation for this very different behaviour in the long-term soot combustion of PrO_2-CP versus CeO_2-CP or PtKBa could be related to the kinetics of oxygen release, since, as observed on Fig. 1c-d, PrO_2-CP presented rather asymmetric patterns of $^{16}O_2$ isotopologue in the oxygen isotopic exchange tests, characterised by long tail, unlike CeO_2-CP or PtKBa with much more

symmetric profiles (see Fig. 1).

Fig. 8 depicts the corresponding $C^{16}O_2$ emission profiles for $Ce_{0.6}Pr_{0.4}O_2$-CP and $Ce_{0.6}Pr_{0.4}O_2$-DC catalysts (and Fig. S6 contains the three CO_2 isotopologue profiles, in arbitrary units, for the sake of comparison). As it was commented above, these two catalysts having the same molar composition in Ce/Pr and very similar BET surface areas, could lead to a more reliable elucidation about the impact of the method of preparation on the soot combustion performance under pulse conditions. As well as PrO_2-CP, the CO_2 emission profiles demonstrate an important contribution of soot combustion during the period under inert atmosphere, which can be referred to as a long tail of CO_2 emission. At the same time, the CO_2 peaks become sharper and more intense (similar to that of CeO_2-CP). Nonetheless, it is obvious the superior soot combustion performance of $Ce_{0.6}Pr_{0.4}O_2$-CP versus $Ce_{0.6}Pr_{0.4}O_2$-DC over the entire range of the experiment after the oxygen pulse. The maximum $C^{16}O_2$ emission rate of $Ce_{0.6}Pr_{0.4}O_2$-CP catalyst reaches a value that is even two times higher than its homologous obtained by the direct calcination method. It was previously discussed that $Ce_{0.6}Pr_{0.4}O_2$-CP presents a slight better atomic homogeneous distribution (between Ce and Pr into the lattice) and this might be the reason of the very different behaviour under pulse conditions. In addition, it is worth noting the higher initial presence of oxygen vacancies in $Ce_{0.6}Pr_{0.4}O_2$-CP, which most likely may favour a higher oxygen interaction, activation and uptake for $Ce_{0.6}Pr_{0.4}O_2$-CP with regard to $Ce_{0.6}Pr_{0.4}O_2$-DC. Accordingly, the two Ce-Pr mixed oxides present different responses in the soot combustion as a function of the method of preparation.

As a following step, all the Ce-Pr mixed oxides were analysed jointly in order to determine the impact of the effect of praseodymium content on their $C^{16}O_2$ emission profiles during soot combustion. For this purpose, Fig. 9 depicts the corresponding $C^{16}O_2$ profiles for each set of ceria-praseodymia catalysts according to the employed method of synthesis. Comparing these sets of catalysts, the same substantial changes in the shape of the profiles are observed from PrO_2 catalyst to Ce-containing catalysts (from $Ce_{0.2}Pr_{0.8}O_2$, $Ce_{0.4}Pr_{0.6}O_2$ to $Ce_{0.6}Pr_{0.4}O_2$, no matter the method of preparation analysed), since the $C^{16}O_2$ emission becomes sharper and more intense after the $^{18}O_2$ pulse, while the same tailing is maintained during the inert period observed for PrO_2 catalysts. All the CO_2 emission profiles of ceria-praseodymia mixed oxides demonstrate a strong improvement in soot combustion performance and the ability to keep this good behaviour in the absence of oxygen, (differently to ceria), what could make its application in gasoline particle filters feasible by increasing the release of oxygen during the long inert periods, after oxygen pulses, typical of the real working conditions of these efficient engines.

For a more complete and accurate view of the catalysts' performances, the $C^{16}O_2$ quantifications were estimated for both first and second pulse of all the catalysts, as shown in Table 5. These quantifications were analysed on the assumption that the soot oxidation produced during the pre-treatment is quite similar between the different tested samples, since at the end of the same pre-treatment only 9–13 %
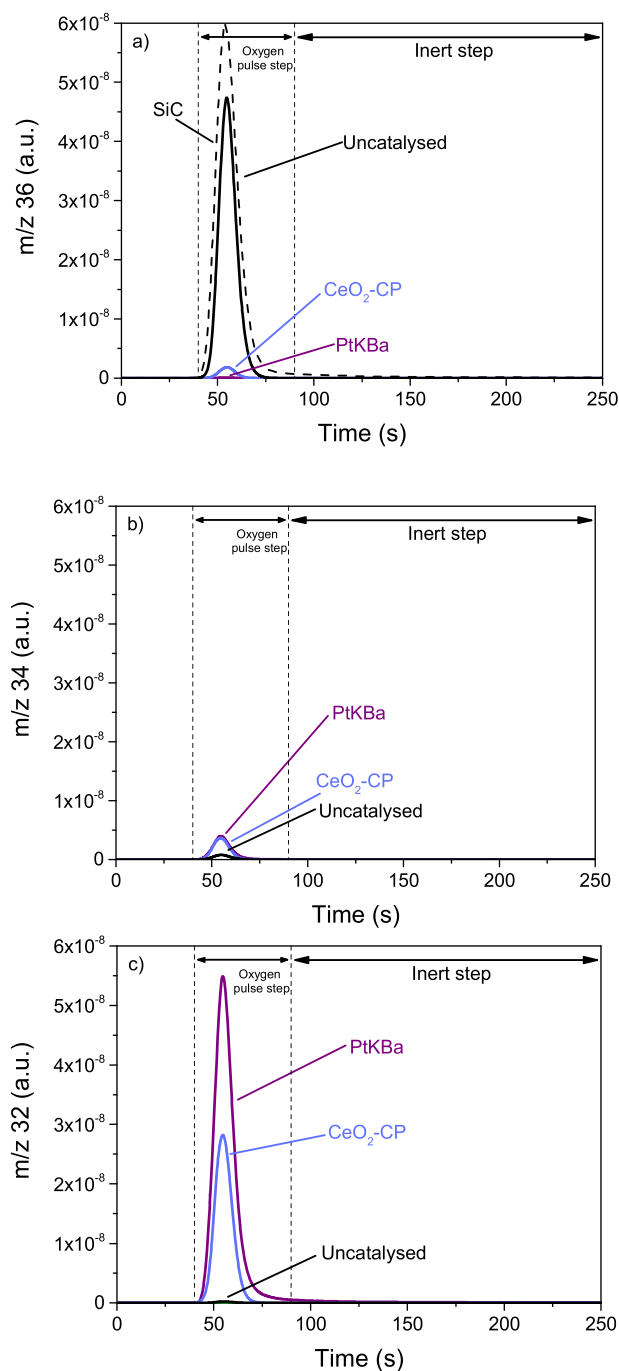
Fig. 7. O_2 isotopologue profiles after injection of the second $^{18}O_2$ pulse over soot-catalyst loose contact mixture at 500 °C under He flow for: a) $^{18}O_2$ isotopologue, b) $^{18}O^{16}O$ isotopologue, and c) $^{16}O_2$ isotopologue. The uncatalysed test has been added for comparative purposes and the corresponding "blank signal" in dotted line.

Fig. 8. Emission of $C^{16}O_2$ isotopologue after injecting the second $^{18}O_2$ pulse over the soot-catalyst loose contact mixture at 500 °C under He flow for $Ce_{0.6}Pr_{0.4}O_2$-CP and $Ce_{0.6}Pr_{0.4}O_2$-DC catalysts.

soot combustion occurred. Therefore, prior to the $^{18}O_2$ injection, (after the pre-treatment in He) some minor changes are expected on the catalysts' surface due to surface oxygen reduction of part of the first monolayer (but a significant surface reconstruction is not expected for these catalysts).

As can be seen, none of the $C^{16}O_2$ emitted values in each pulse overcome the corresponding value of oxygen injected per pulse (23.7 μmol $^{18}O_2$/g$_{cat}$). This suggests a certain "misuse" of the employed oxygen in order to burn the soot in the presence of the catalyst. Interestingly, the utilisation ratios of the $^{18}O_2$ pulses to yield CO_2 cover a
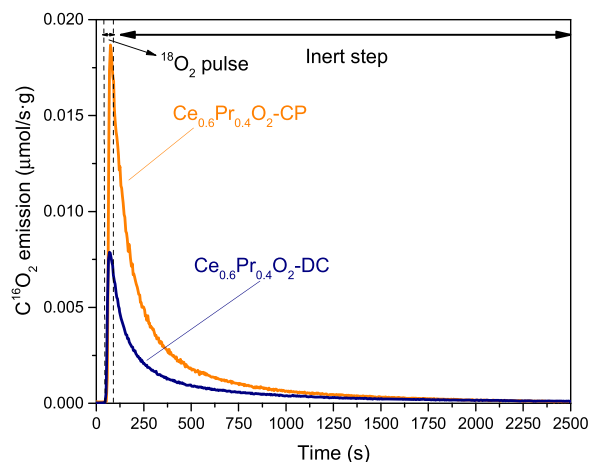
wide range of values for the catalysed reaction (from a 17.3 % value, obtained with the Pt-catalyst, to an 82.8 % value, obtained with the $Ce_{0.2}Pr_{0.8}O_2$-DC catalyst), proving evidence of a high effectivity of these proposed catalysts towards the soot combustion under O_2 pulsed mode, and in turn, on their potential for this demanding application. On the other hand, despite of the highest BET surface area of CeO_2-CP, its utilisation ratio is moderate (29.1 %), clearly inferior to whatever estimated for the Pr-containing samples. In order to understand this poor performance, it is necessary to take into account two important factors. Firstly, labelled oxygen emissions ($^{18}O_2$ and $^{18}O^{16}O$), and the unlabelled one ($^{16}O_2$) were observed at the first stages of the oxygen injection only for CeO_2-CP (see Fig. 7a, b, c), implying that all the exchanged oxygen cannot be effectively used for the soot combustion purpose. On the other hand, this catalyst (unlike ceria-praseodymia mixed oxides) does not present a significant soot combustion during the inert period, therefore the supplied oxygen seems to be effective during the short period of the pulse.

Focussing on the very active ceria-praseodymia mixed oxides, it can be stated that the CP-catalysts seem to exhibit higher soot combustion activities than their counterparts prepared by means of the DC-method. However, and due possibly to the decrease in the BET surface area as the Pr loading increases in the mixed oxides, the soot combustion activity is approximately kept constant in the series ($Ce_{0.6}Pr_{0.4}O_2$-CP; $Ce_{0.4}Pr_{0.6}O_2$-CP; $Ce_{0.2}Pr_{0.8}O_2$-CP). This effect can be interpreted as a result of the balance among the benefits of increasing the Pr content and the disadvantages of the decrease in the BET surface area. This tentative interpretation seems to be confirmed by the gradual increase in soot combustion activities with the Pr content for the DC-series (in which the BET surface areas exhibit minor changes). A previously stated, the influence of the method of preparation on the soot combustion activity cannot be systematised and explained in a smooth way due to the fact that the BET surface areas do not exhibit the same trends or variations in terms of the Pr contents along every series.

4. Conclusion

The main conclusions of this study concerning the oxygen interaction and soot combustion over three model catalysts (two bare oxides and a Pt-based catalysts) along with two sets of ceria-praseodymia catalysts with pulse experiments using $^{18}O_2$ are as follows:

A novel methodology for the analysis of the oxygen activation and uptake capacity over a considerable number of catalysts, (by means of pulse experiments with isotopic $^{18}O_2$), is presented for the first time. This methodology simulates the oxygen pulse conditions existing in a
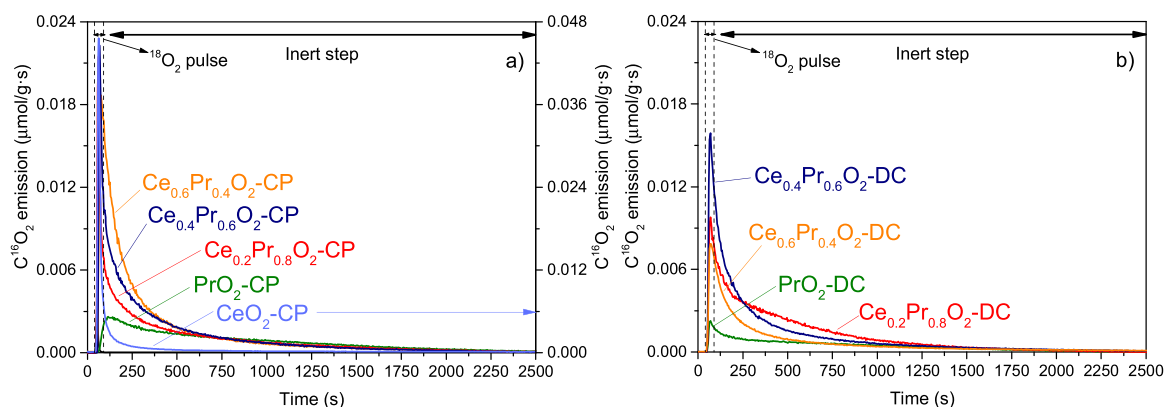
Fig. 9. Emission of $C^{16}O_2$ isotopologue after injecting the second $^{18}O_2$ pulse over the soot-catalyst loose contact mixture at 500 °C under He flow for ceria-praseodymia catalysts obtained by: a) co-precipitation method and b) direct calcination method.

Table 5
Quantifications estimated of the emission of $C^{16}O_2$ isotopologue for all the catalysts investigated after the first and the second $^{18}O_2$ pulse.

Catalyst	$C^{16}O_2$ emitted (µmol CO_2/g_{cat})			Utilisation[a] ratios of the $^{18}O_2$ pulses (%)
	1st pulse	2nd pulse	Total[b]	
CeO$_2$-CP	7.0	6.7	13.8	29.1
PtKBa	5.0	3.2	8.2	17.3
PrO$_2$-CP	14.7	15.6	30.3	63.9
Ce$_{0.2}$Pr$_{0.8}$O$_2$-CP	17.0	18.2	35.1	74.1
Ce$_{0.4}$Pr$_{0.6}$O$_2$-CP	17.2	18.7	35.9	75.7
Ce$_{0.6}$Pr$_{0.4}$O$_2$-CP	17.0	18.7	35.7	75.3
PrO$_2$-DC	9.4	10.4	19.8	41.8
Ce$_{0.2}$Pr$_{0.8}$O$_2$-DC	18.8	20.4	39.2	82.7
Ce$_{0.4}$Pr$_{0.6}$O$_2$-DC	16.2	17.7	33.9	71.5
Ce$_{0.6}$Pr$_{0.4}$O$_2$-DC	8.4	9.6	18.0	38.0
Uncatalysed soot combustion[c]	0.3	0.1	0.4	0.84

[a] Comparative calculations about how much of the $^{18}O_2$ pulses is converted to CO_2 (assuming that $C^{18}O^{16}O$ and $C^{18}O_2$ are negligible compared to the $C^{16}O_2$ emission, which is strictly valid for all the catalysed reactions, and on the basis that every pulse injected consists of 23.7 µmol $^{18}O_2$/g_{cat}).

[b] These quantifications were analysed on the assumption that the soot oxidation produced during the pre-treatment is quite similar between the different tested samples (excluding the Pt-catalyst), since only 9–13 % soot combustion takes place, as average value during the pre-treatment at 500 °C under He.

[c] Not strictly comparable in absolute terms since $C^{16}O_2$ is not the only isotopologue emitted for the case of the uncatalysed reaction.

GDI exhaust.

Among the model catalysts selected, pure PrO$_2$ presents a remarkable activity to interact with the oxygen pulse (since very low temperatures) and uptake oxygen. These interesting abilities were connected with its capacity to evolve oxygen under inert atmosphere. Conversely, the Pt-catalyst does not exhibit any oxygen uptake under these experimental conditions.

Pr-containing samples are much more active concerning activation and interaction with the $^{18}O_2$ pulses (even than pure ceria), despite of their lower BET surface areas.

Ce-Pr mixed oxides present different responses in the O$_2$ activation, uptake and exchange processes, as a function of temperature, praseodymium content and, mainly, method of preparation. Interestingly, the co-precipitated samples (whatever the BET surface area that possess) are characterised by high levels of $^{18}O_2$ consumption at the beginning of the experiments and high levels of oxygen uptakes if compared with those of the direct-calcination catalysts.

The comparison among the impact of the preparation method taking one fixed Ce/Pr composition (Ce$_{0.6}$Pr$_{0.4}$O$_2$, because both catalysts present similar BET surface areas) allowed us to suggest that a best atomic homogeneity and a higher population of oxygen vacancies might be behind the best response of Ce$_{0.6}$Pr$_{0.4}$O$_2$ prepared by the co-precipitation method if compared with its counterpart prepared by the direct calcination method.

All the catalysts yield mainly $C^{16}O_2$ isotopologue as majority soot combustion product at 500 °C, evidencing that the active oxygen species come from the catalysts and are transferred to the soot surface. $^{18}O_2$ pulses filled up the possible vacancies created.

$C^{16}O_2$ emerges with very different profiles depending on Ce/Pr composition. CeO$_2$ is characterised by a sharp and intense CO$_2$ peak during the own $^{18}O_2$ pulse, however the intervention of unlabelled active oxygen species during the inert period after the pulse is not very marked. As more and more Pr is incorporated into the mixed oxide's formulation, the intervention of the oxygen species during the long inert period is more relevant. As a consequence of this, the best formulations seem to be the Ce-Pr mixed oxides with high Pr content. This influence is seen clearly for the direct calcination method. Unfortunately, the loss in BET surface area for the catalysts prepared by the co-precipitation method reduces the benefits of employing this route of preparation.

Ceria-praseodymia mixed oxides have proven to be excellent candidates for soot oxidation under the demanding conditions of GDI exhaust, as they combine a high reactivity during the own $^{18}O_2$ pulse and the long-term activity during the long inert period.

CRediT authorship contribution statement

J.C. Martínez-Munuera: Conceptualization, Methodology, Investigation, Validation, Visualization, Writing – original draft. **M. Cortés-Reyes**: Methodology, Investigation, Validation, Visualization. **A. García-García:** Conceptualization, Methodology, Validation, Visualization, Writing – original draft, Supervision, Funding acquisition.

Declaration of Competing Interest

The authors declare that they have no known competing financial interests or personal relationships that could have appeared to influence the work reported in this paper.

Data availability

No data was used for the research described in the article.

Acknowledgements

Appendix A. Supporting information

Supplementary data associated with this article can be found in the online version at doi:10.1016/j.apcatb.2023.122525.

References

[1] A. Joshi, Review of vehicle engine efficiency and emissions, SAE Int. J. Adv. Curr. Pr. Mobil. 2 (2020) 2479–2507.

[2] P. Nicolin, D. Rose, F. Kunath, T. Boger, Modeling of the soot oxidation in gasoline particulate filters, SAE Tech. Pap. 2015 (2015) 01–1048.

[3] T.V. Johnson, Review of emerging trends on gasoline emissions control, in: Proceedings of the Third International Conference Advanced Emission Control Concepts for Gasoline Engines, May 2014 (2014).

[4] International Agency for Research on Cancer: Outdoor Air Pollution a Leading Environmental Cause of Cancer Deaths, 2013. Press Release N° 221.

[5] C. Liu, R. Chen, F. Sera, A.M. Vicedo-Cabrera, Y. Guo, S. Tong, M.S.Z.S. Coelho, P. H.N. Saldiva, E. Lavigne, P. Matus, N. Valdes Ortega, S. Osorio Garcia, M. Pascal, M. Stafoggia, M. Scortichini, M. Hashizume, Y. Honda, M. Hurtado-Díaz, J. Cruz, B. Nunes, J.P. Teixeira, H. Kim, A. Tobias, C. Íñiguez, B. Forsberg, C. Åström, M. S. Ragettli, Y.-L. Guo, B.-Y. Chen, M.L. Bell, C.Y. Wright, N. Scovronick, R. M. Garland, A. Milojevic, J. Kyselý, A. Urban, H. Orru, E. Indermitte, J.J. K. Jaakkola, N.R.I. Ryti, K. Katsouyanni, A. Analitis, A. Zanobetti, J. Schwartz, J. Chen, T. Wu, A. Cohen, A. Gasparrini, H. Kan, Ambient particulate air pollution and daily mortality in 652 cities, N. Engl. J. Med. 381 (2019) 705–715.

[6] A. Joshi, T.V. Johnson, Gasoline particulate filters—a review, Emiss. Control Sci. Technol. 4 (2018) 219–239.

[7] S. Liu, X. Wu, W. Liu, W. Chen, R. Ran, M. Li, D. Weng, Soot oxidation over CeO_2 and Ag/CeO_2: factors determining the catalyst activity and stability during reaction, J. Catal. 337 (2016) 188–198.

[8] E. Aneggi, A. Trovarelli, Potential of ceria-zirconia-based materials in carbon soot oxidation for gasoline particulate filters, Catalysts 10 (2020) 768.

[9] T. Boger, D. Rose, P. Nicolin, N. Gunasekaran, T. Glasson, Oxidation of soot (Printex® U) in particulate filters operated on gasoline engines, Emiss. Control Sci. Technol. 1 (2015) 49–63.

[10] S. Liu, X. Wu, D. Weng, R. Ran, Ceria-based catalysts for soot oxidation: a review, J. Rare Earth 33 (2015) 567–590.

[11] N. Guillén-Hurtado, A. Bueno-López, A. García-García, Catalytic performances of ceria and ceria-zirconia materials for the combustion of diesel soot under NO_x/O_2 and O_2. Importance of the cerium precursor salt, Appl. Catal. A Gen. 437–438 (2012) 166–172.

[12] J. Giménez-Mañogil, A. García-García, Opportunities for ceria-based mixed oxides versus commercial platinum-based catalysts in the soot combustion reaction. Mechanistic implications, Fuel Process. Technol. 129 (2015) 227–235.

[13] N. Guillén-Hurtado, A. García-García, A. Bueno-López, Active oxygen by Ce–Pr mixed oxide nanoparticles outperform diesel soot combustion Pt catalysts, Appl. Catal. B 174–175 (2015) 60–66.

[14] J.C. Martínez-Munuera, M. Zoccoli, J. Giménez-Manogil, A. García-García, Lattice oxygen activity in ceria-praseodymia mixed oxides for soot oxidation in catalysed Gasoline Particle Filters, Appl. Catal. B 245 (2019) 706–720.

[15] W.Y. Hernandez, M.N. Tsampas, C. Zhao, A. Boreave, F. Bosselet, P. Vernoux, La/Sr-based perovskites as soot oxidation catalysts for Gasoline Particulate Filters, Catal. Today 258 (2015) 525–534.

[16] W.Y. Hernandez, D. Lopez-Gonzalez, S. Ntais, C. Zhao, A. Boreave, P. Vernoux, Silver-modified manganite and ferrite perovskites for catalyzed gasoline particulate filters, Appl. Catal. B 226 (2018) 202–212.

[17] W. Yang, S. Wang, K. Li, S. Liu, L. Gan, Y. Peng, J. Li, Highly selective α-Mn_2O_3 catalyst for cGPF soot oxidation: surface activated oxygen enhancement via selective dissolution, Chem. Eng. J. 364 (2019) 448–451.

[18] Y.X. Gao, A.Q. Duan, S. Liu, X.D. Wu, W. Liu, M. Li, S.G. Chen, X. Wang, D. Weng, Study of $Ag/Ce_xNd_{1-x}O_2$ nanocubes as soot oxidation catalysts for gasoline particulate filters: balancing catalyst activity and stability by Nd doping, Appl. Catal. B Environ. 203 (2017) 116–126.

[19] H.L. Wang, S. Liu, Z. Zhao, X. Zou, M.H. Liu, W. Liu, X.D. Wu, D. Weng, Activation and deactivation of Ag/CeO_2 during soot oxidation: influences of interfacial ceria reduction, Catal. Sci. Technol. 7 (2017) 2129–2139.

[20] H. Wang, B. Jin, H. Wang, N. Ma, W. Liu, D. Weng, X. Wu, S. Liu, Study of Ag promoted $Fe_2O_3@CeO_2$ as superior soot oxidation catalysts: the role of Fe_2O_3 crystal plane and tandem oxygen delivery, Appl. Catal. B 237 (2018) 251–262.

[21] S. Liu, X.D. Wu, J. Tang, P.Y. Cui, X.Q. Jiang, C.G. Chang, W. Liu, Y.X. Gao, M. Li, D. Weng, An exploration of soot oxidation over CeO_2-ZrO_2 nanocubes: do more surface oxygen vacancies benefit the reaction? Catal. Today 281 (2017) 454–459.

[22] X. Wang, B. Jin, R. Feng, W. Liu, D. Weng, X. Wu, S. Liu, A robust core-shell silver soot oxidation catalyst driven by Co_3O_4: effect of tandem oxygen delivery and Co_3O_4-CeO_2 synergy, Appl. Catal. B 250 (2019) 132–142.

[23] R. Ashikaga, K. Murata, T. Ito, Y. Yamamoto, S. Arai, A. Satsuma, Tuning the oxygen release properties of CeO_2-based catalysts by metal–support interactions for improved gasoline soot combustion, Catal. Sci. Technol. 10 (2020) 7177–7185.

[24] H. Liang, B. Jin, M. Li, X. Yuan, J. Wan, W. Liu, X. Wu, S. Liu, Highly reactive and thermally stable Ag/YSZ catalysts with macroporous fiber-like morphology for soot combustion, Appl. Catal. B 294 (2021), 120271.

[25] M. Machida, Y. Murata, K. Kishikawa, D. Zhang, K. Ikeue, On the reasons for high activity of CeO_2 catalyst for soot oxidation, Chem. Mater. 20 (2008) 4489–4494.

[26] R. Möller, M. Votsmeier, C. Onder, L. Guzzella, J. Gieshoff, Is oxygen storage in three-way catalysts an equilibrium controlled process? Appl. Catal. B 91 (2009) 30–38.

[27] P. Piqueras, E.J. Sanchis, J.M. Herreros, A. Tsolakis, Evaluating the oxidation kinetic parameters of gasoline direct injection soot from thermogravimetric analysis experiments, Chem. Eng. Sci. 234 (2021), 116437.

[28] D. Fino, S. Bensaid, M. Piumetti, N. Russo, A review on the catalytic combustion of soot in diesel particulate filters for automotive applications: from powder catalysts to structured reactors, Appl. Catal. A 509 (2016) 75–96.

[29] M. Cortés-Reyes, M.C. Herrera, I.S. Pieta, M.A. Larrubia, L.J. Alemany, In situ TG-MS study of NOx and soot removal over LNT model catalysts, Appl. Catal. A Gen. 523 (2016) 193–199.

[30] M. Cortés-Reyes, C. Herrera, M.A. Larrubia, L.J. Alemany, Intrinsic reactivity analysis of soot removal in LNT-catalysts, Appl. Catal. B Environ. 193 (2016) 110–120.

[31] N. Guillén-Hurtado, A. García-García, A. Bueno-López, Isotopic study of ceria-catalyzed soot oxidation in the presence of NO_x, J. Catal. 332 (2013) 181–187.

[32] A. Bueno-López, K. Krishna, B. van der Linden, G. Mul, J.A. Moulijn, M. Makkee, On the mechanism of model diesel soot-O_2 reaction catalysed by Pt-containing La^{3+}-doped CeO_2: a TAP study with isotopic O_2, Catal. Today 121 (2007) 237–245.

[33] A. Bueno-López, K. Krishna, M. Makkee, J.A. Moulijn, Active oxygen from CeO_2 and its role in catalysed soot oxidation, Catal. Lett. 99 (2005) 203–205.

[34] K. Klier, J. Nokanova, P. Jiru, Exchange reactions of oxygen between oxygen molecules and solid oxides, J. Catal. 2 (1963) 479–484.

[35] V.S. Muzykantov, V.S. Popovski, G.K. Boreskov, Kinetics of isotope exchange in a molecular oxygen—solid oxide system, Kinet. Katal. 5 (1964) 624–629.

[36] E.M. Sadovskaya, A.S. Bobin, V.V. Skazka, Isotopic transient analysis of oxygen exchange over oxides, Chem. Eng. J. 348 (2018) 1025–1036.

[37] C.-Y. Yoo, H.J.M. Bouwmeester, Oxygen surface exchange kinetics of $SrTi_{1-x}Fe_xO_{3-\delta}$ mixed conducting oxides, Phys. Chem. Chem. Phys. 14 (2012) 11759–11765.

[38] S. Saher, J. Song, V. Vibhu, C. Nicollet, A. Flura, J.-M. Bassat, H.J.M. Bouwmeester, Influence of annealing at intermediate temperature on oxygen transport kinetics of $Pr_2NiO_{4+\delta}$, J. Mater. Chem. A 6 (2018) 8331–8339.

[39] C.-Y. Yoo, B.A. Boukamp, H.J.M. Bouwmeester, Oxygen surface exchange kinetics on $PrBaCo_2O_{5+\delta}$, Solid State Ion. 262 (2014) 668–671.

[40] Y. Madier, C. Descorme, A.M. Le Govic, D. Duprez, Oxygen mobility in CeO_2 and $Ce_xZr_{(1-x)}O_2$ compounds: study by CO transient oxidation and $^{18}O/^{16}O$ isotopic exchange, J. Phys. B 103 (1999) 10999–11006.

[41] H.C. Yao, Y.F. Yu Yao, Ceria in automotive exhaust catalysts: I. Oxygen storage, J. Catal. 86 (1984) 254–265.

[42] C. Li, K. Domen, K. Maruya, T. Onishi, Dioxygen adsorption on well-outgassed and partially reduced cerium oxide studied by FT-IR, J. Am. Chem. Soc. 111 (1989) 7683–7687.

[43] C. Li, K. Domen, K. Maruya, T. Onishi, Oxygen exchange reactions over cerium oxide: an FT-IR study, J. Catal. 123 (1990) 436–442.

[44] M. Cortés-Reyes, C. Herrera, M.A. Larrubia, L.J. Alemany, Understanding of soot removal mechanism over DeNOx-catalysts as passive converters, Ind. Eng. Chem. Res. 60 (2021) 6501–6511.

[45] L. Castoldi, R. Matarrese, L. Lietti, P. Forzatti, Intrinsic reactivity of alkaline and alkaline-earth metal oxide catalysts for oxidation of soot, Appl. Catal. B 90 (2009) 278–285.

[46] J. Jung, J.H. Lee, S. Song, M. Chun, Measurement of soot oxidation with NO_2-O_2-H_2O in a flow reactor simulating diesel engine DPF, Int. J. Automot. 9 (2008) 423–428.

[47] C. Arnal, M.U. Alzueta, A. Millera, R. Bilbao, Experimental and kinetic study of the interaction of a commercial soot with NO at high temperature, Combust. Sci. Technol. 184 (2012) 1191–1206.

[48] L. Soler, A. Casanovas, C. Escudero, V. Pérez-Dieste, Eleonora Aneggi, A. Trovarelli, J. Llorca, Ambient pressure photoemission spectroscopy reveals the mechanism of carbon soot oxidation in ceria-based catalysts, ChemCatChem 8 (2016) 2748–2751.

[49] A. Bueno-López, Diesel soot combustion ceria catalysts, Appl. Catal. B 146 (2014) 1–11.

[50] N. Guillén-Hurtado, J. Giménez-Mañogil, J.C. Martínez-Munuera, A. Bueno-López, A. García-García, Study of Ce/Pr ratio in ceria-praseodymia catalysts for soot combustion under different atmospheres, Appl. Catal. A Gen. 590 (2020), 117339.